Available online at www.sciencedirect.com
SCIENCE DIRECT®
Vision Research 45 (2005) 1107–1114
Vision Research
www.elsevier.com/locate/visres

Effect of hypercholesterolemia on inducible nitric oxide synthase expression in a rat model of elevated intraocular pressure

İclal Yücel [a], Yusuf Akar [a], Gültekin Yücel [b], M. Akif Çiftçioğlu [c], Nuran Keleş [c], Mutay Aslan [b,*]

[a] Department of Ophthalmology, Akdeniz University Medical School, 07070 Antalya, Turkey
[b] Department of Biochemistry, Akdeniz University Medical School, 07070 Antalya, Turkey
[c] Department of Pathology, Akdeniz University Medical School, 07070 Antalya, Turkey

Received 19 August 2004; received in revised form 5 October 2004

Abstract

Purpose: This study was performed to examine the effect of hypercholesterolemia on inducible nitric oxide synthase (NOS-2) expression and oxidative tissue injury in an experimental rat model of elevated IOP. *Methods*: Wistar rats were maintained on either regular chow or a high-cholesterol diet for 24 weeks. Intraocular pressure (IOP) was elevated in hypercholesterolemic rats by unilaterally cauterizing three episcleral vessels. Rats were divided into four experimental groups as follows; hypercholesterolemia, hypercholesterolemia + elevated IOP, elevated IOP and control. NOS-2 distribution, lipid peroxidation and retinal nerve fiber layer (RNFL) thickness was evaluated in all experimental groups at the end of 24 weeks. *Results*: Light microscopic evaluation of retinas in hypercholesterolemic rats revealed breaks and discontinuation in focal areas in the outer nuclear layer (ONL). NOS-2 positive staining was observed throughout the outer plexiform layer (OPL), inner plexiform layer (IPL) and ganglion cell layer (GCL) in rats with elevated IOP and/or hypercholesterolemia. Calculated values of RNFL thickness in hypercholesterolemic rats were significantly higher than those in the control and elevated IOP group. Vitreous malondialdehyde (MDA) levels detected in elevated IOP (3.51 ± 0.31 nmol/mg protein) and hypercholesterolemia + elevated IOP (5.14 ± 1.28 nmol/mg protein) groups were significantly higher than those detected in hypercholesterolemic (1.92 ± 1.43 nmol/mg protein) and control (1.89 ± 0.24 nmol/mg protein) groups. *Conclusion*: The presented data confirms hypercholesterolemia as a risk factor in the development of glaucomatous optic neuropathy (GON) and suggests that increased circulating cholesterol may exacerbate disease progression by inducing NOS-2 expression and elevating oxidant tissue injury.

Abbreviations: GCL, ganglion cell layer; GON, glaucomatous optic neuropathy; IOP, intraocular pressure; IPL, inner plexiform layer; MDA, malondialdehyde; NMDA, *N*-methyl-D-aspartate; NO, nitric oxide; NOS-2, inducible nitric oxide synthase; O_2^-, superoxide; ONL, outer nuclear layer; $ONOO^-$, peroxynitrite; OPL, outer plexiform layer; RNFL, retinal nerve fiber layer; ROS, reactive oxygen species; TBA, thiobarbituric acid; VCL, photoreceptor cell layer

Keywords: Glaucoma; Hypercholesterolemia; Nitric oxide synthase

1. Introduction

Glaucoma is a progressive optic neuropathy characterized by optic disc and nerve fiber layer damage. Although the pathophysiological mechanisms leading to GON remain uncertain, mechanical compression and vascular ischemia have been suggested to play a

* Corresponding author. Tel.: +90 242 2274343/44126; fax: +90 242 2274482.
E-mail address: mutayaslan@akdeniz.edu.tr (M. Aslan).

0042-6989/$ - see front matter © 2004 Elsevier Ltd. All rights reserved.
doi:10.1016/j.visres.2004.11.018

leading role in the observed neuronal damage (Fechtner & Weinreb, 1994). The mechanical compression theory considers elevated IOP as the most important risk factor for the disease (Yan, Coloma, & Metheetrairut, 1994). This theory gives support to the essential signs of glaucomatous optic neuropathy, such as increased cupping (Greenfield, 1999) and neuroretinal rim thinning (Jonas, Budde, & Lang, 1998) but does not explain the existence of normal tension glaucoma (Yamamoto & Kitazawa, 1998). Alternatively, the vascular ischemia theory supposes that vascular insufficiency in the optic nerve head results in decreased metabolic activity which subsequently leads to increased glutamate accumulation and ganglion cell death (Flammer, 1994; Sucher, Lipton, & Dreyer, 1997). Indeed, a large number of studies have shown a high association between GON and vascular disorders related to hypertension, diabetes and hypercholesterolemia (Hayreh, Bill, & Sperber, 1994; Hayreh, Pe'er, & Zimmerman, 1999; Hennis, Wu, & Nemesure, 2003; Klein, Klein, & Moss, 1984; McGwin et al., 2004; Stewart, Sine, Sutherland, & Stewart, 1996; Tanaka, Yamazaki, & Yokoyama, 2001; Winder, 1977).

Increased glutamate accumulation resulting from vascular insufficiency can reach potentially toxic levels when released synaptically. Glutamate is an excitatory neurotransmitter which acts on *N*-methyl-D-aspartate (NMDA) receptors located in the plasma membrane of both neurons and glia (Sucher et al., 1997). Overstimulation of NMDA receptors increases intracellular calcium to toxic levels and activates nitric oxide synthase (NOS), resulting in excessive nitric oxide (NO) production (Montoliu, Llansola, & Monfort, 2001). Nitric oxide-mediated cytotoxicity and the capacity of NO to induce apoptosis have been documented in macrophages (Sarih, Souvannavong, & Adam, 1993) astrocytes (Hu & Van Eldik, 1996) and neuronal cells (Heneka et al., 1998). Although the mechanisms of NO-mediated apoptosis are not clearly elucidated, the induction of apoptosis by NO can be the result of DNA damage which in turn activates p53 that has been reported to cause apoptosis (Kim, Bombeck, & Billiar, 1999).

Nitric oxide exhibits a wide spectrum of functions in both normal and pathological states. Physiological amounts of NO synthesized by constitutive NOS isoforms (NOS-1 and NOS-3) participates in neurotransmission and cardiovascular signaling (Goldstein, Ostwald, & Roth, 1996) while excessive amounts of NO released by NOS-2 (Becquet, Courtois, & Goureau, 1997) results in cytotoxicity via reacting with superoxide ($O_2^{\cdot-}$) to form the potent oxidant peroxynitrite ($ONOO^-$) (Beckman, Beckman, & Chen, 1990). Recent studies have highlighted the role of NO in GON by reporting the presence of NOS-2 in glaucomatous optic nerve heads of rat (Shareef, Sawada, & Neufeld, 1999) and humans (Liu & Neufeld, 2000).

Based on studies reporting hypercholesterolemia as a risk factor for elevated IOP (Hayreh et al., 1994; Hayreh et al., 1999; McGwin et al., 2004; Stewart et al., 1996; Tanaka et al., 2001; Winder, 1977) and on data showing NOS-2 expression in the optic nerves of rats with chronic moderately elevated IOP (Shareef et al., 1999), we wanted to determine the effect of hypercholesterolemia on NOS-2 expression in an experimental rat model of elevated IOP. Hence, the purpose of this study was to examine the retinal distribution and content of NOS-2 in hypercholesterolemic rats that have undergone episcleral venous occlusion. The extent of retinal damage was quantified histologically by measuring RNFL thickness, while NO-mediated cytotoxicity was assessed via measuring vitreous lipid oxidation in all experimental groups.

2. Materials and methods

2.1. Animals

All experimental protocols conducted on rats were performed in accordance with the standards established by the Institutional Animal Care and Use Committee at Akdeniz University Medical School. Male Wistar rats weighing 350–450 g were housed in spacious cages and given food and water ad libitum. Animals were maintained at 12 h light-dark cycles and a constant temperature of 23 ± 1 °C at all times. Rats were divided into four groups of 15 animals each; Group 1: hypercholesterolemia, Group 2: hypercholesterolemia + elevated IOP, Group 3: elevated IOP, Group 4: control.

2.2. Experimental hypercholesterolemia

Hypercholesterolemia was induced by feeding rats with laboratory chow supplemented with 4% (w/w) cholesterol, 1% cholic acid and 0.5% thiouracil for 24 weeks (Aliev, Shi, & Perry, 2000). All animals were sacrificed at the end of 24 weeks and blood samples were collected via intracardiac puncture. Serum cholesterol levels were assayed by an automatic analyzer (Hitachi-911) using Boehringer-Mannheim kits (Mannheim, Germany).

2.3. Rat model of elevated IOP

IOP was elevated in rats by unilaterally cauterizing three episcleral vessels, as previously (Sawada & Neufeld, 1999; Shareef, Garcia-Valenzuela, & Salierno, 1995) described. Briefly, rats were anesthetized intraperitoneally with a mixture of ketamine hydrochloride (15 mg/kg), xylazine hydrochloride (0.3 mg/kg) and acepromazine (1.5 mg/kg). Episcleral vessels were exposed by incising the overlying conjunctiva and cauterized

via an ophthalmic cautery. IOP was measured before surgery, on the 7th and 15th days after surgery and once a month over a 6 month period. A handheld tonometer (XL-Tonopen, Mentor O and O, Norwell, MA, USA) was used to measure IOP in rats under light anesthesia induced by 3 mg/kg acepromazine. One drop of 0.5% proparacaine hydrochloride was applied to each eye before readings were obtained. Intraocular pressure measurements were performed as described in the instruction manual of the tonometer. The mean IOP of 5–10 consecutive measurements were recorded. Episcleral venous occlusion in hypercholesterolemic rats was formed on the 60th day following the initiation of hypercholesterolemic diet.

2.4. Measurement of retinal nerve fiber layer thickness

Globes were enucleated at the end of the experimental period and sectioned in the vertical meridian. Obtained samples were prefixed in 2.2% glutaraldehyde in 0.1 M (pH 7.4) Sorensen's phosphate buffer for 4 h and postfixed in 1% osmium tetroxide (0.1 M, pH 7.2) for 1 h. The samples were dehydrated in graded ethyl alcohol series and embedded in Araldite CY212. Semithin sections were stained with toluidine blue and observed by Nikon opthipot light microscope. RNFL thickness measurements were standardized by selecting the same topographic region of the retina in all experimental groups. All measurements were performed at the central retina, within 1 mm from the optic nerve margin. Retinal NFL thickness measurements were performed in a double-blinded fashion.

2.5. Measurement of lipid peroxidation

Vitreous was harvested from enucleated globes and stored at −80 °C until analyzed. The liquefied vitreus was centrifuged at $14{,}000 \times g$ to remove cellular debris. Obtained supernatants were transferred to clean tubes and used for lipid peroxidation analysis. Levels of MDA, a product of lipid peroxidation, was measured using the thiobarbituric acid (TBA) fluorometric assay (Wasowicz, Neve, & Peretz, 1993) with 1,1,3,3-teraethoxypropane as a standard. Briefly, 50 μl of tissue sample was added to 1 ml distilled water which was then mixed with equal volumes of 29 mM TBA in acetic acid. After 1 h incubation at >95 °C, samples were cooled and 25 μl of 5 mM HCL was added. The final reaction mixture was extracted with 3.5 ml of n-butanol and the butanol phase was separated via centrifugation at $1500 \times g$ for 5 min. MDA levels were determined fluorometrically with excitation and emission wavelengths of 532 nm and 547 nm, respectively. Protein concentrations in all samples were measured spectrophotometrically by a Lowry assay (Lowry, Rosenbrough, & Farr, 1951) with bovine serum albumin as a standard.

2.6. Immunohistochemical staining

Enucleated globe materials were fixed in 10% buffered formalin solutions and incised in transverse plain just from the center of the globe to obtain two equal parts. Fixed tissues were washed in phosphate buffered saline (pH 7.4), embedded in paraffin and cut into 4-μm sections. For the peroxidase staining procedure sections were deparaffined, rehydrated and washed with 0.1 M glycine-Tris solution. To block nonspecific binding, the tissue sections were preincubated with 2% goat serum at room temperature for 30 min. Primary antibody incubations were for 60 min at 25 °C using rabbit polyclonal anti-NOS2 (1:100 dilution, Santa Cruz Biotechnology, Santa Cruz, CA). After sections were washed they were immunostained with an avidin–biotin complex kit (Dako, Glostrup, Denmark) followed by hematoxylin counterstaining. Negative controls were performed by replacing the primary antibody with nonimmune serum followed by immunoperoxidase staining.

Presence of a red–brown colored end-product in the cytoplasm was indicative of positive staining. Counterstaining with hematoxylin resulted in a pale to dark blue coloration of cell nuclei. To obtain a quantitative standard for NOS-2 immunostaining within the different experimental group's morphometric analysis was performed on all retinal sections by a pathologist blinded to the experimental conditions. The immunostaining scores, obtained according to both the percentage and intensity of positive stained cells, were statistically analyzed by Sigma Stat (version 2.03) software for windows. The percentage of the positive stained cells was scored as follows: 0 = less than 5% of the cells/high powered field (HPF, 40×) are stained, 1 = 5% to less than 30% of cells/HPF are stained. 2 = 30% to less than 50% of cells/HPF are stained. 3 = more than 50% of cells/HPF are stained. The intensity of staining within each counted cell was also scored as follows: 0 = no staining, 1 = weak staining (pale red–brown), 2 = moderate staining (red–brown), 3 = strong staining (dark red–brown). A final immunostaining score was obtained for all sections by adding the two scores.

2.7. Statistical analysis

The statistical analysis of the obtained data was performed by Sigma Stat (version 2.03) software for windows. The differences in the MDA values and immunostaining scores among the different groups were analyzed via Kruskal–Wallis one way analysis of variance on ranks and all pairwise multiple comparisons were performed by Dunn's Method. The differences in the RNFL thickness and cell numbers among the different groups were analyzed via one way analysis of variance and all pairwise multiple comparisons were performed by Tukey Test. The calculated p values by

the Sigma Stat (version 2.03) statistical software program are given as $p < 0.01$, $p < 0.05$ or $p < 0.001$.

3. Results

3.1. Cholesterol and IOP levels

Cholesterol levels (mean ± SD, $n = 15$) were significantly greater ($p < 0.01$) in rats fed on cholesterol-enriched diet than those fed on standard chow (190 ± 11 mg/dL and 70 ± 5 mg/dL, respectively). The IOP (mean ± SD, $n = 15$) measured in control eyes were 10 ± 1.1 mm Hg. An increase of 7–10 mm Hg was observed in cauterized eyes compared to contralateral controls. Recorded IOP from cauterized eyes remained elevated over the 6 month experimental period.

3.2. Retinal nerve fiber layer thickness

RNFL thickness in hypercholesterolemic rats were significantly higher ($p < 0.01$) than those in the control and elevated IOP groups (Fig. 1). Calculated values (mean ± SD, $n = 9$) of RNFL thickness in the experimental groups were as follows, control: 25.1 ± 1.28 μm, hypercholesterolemia: 31.6 ± 1.26 μm, elevated IOP: 25.3 ± 1.49 μm, hypercholesterolemia + elevated IOP: 32.1 ± 2.6 μm. No significant change in RNFL thickness was found in the elevated IOP group after 24 weeks following surgery.

3.3. Histologic analysis

Fig. 2 illustrates photomicrographs of retinal cross sections from representative rats of each of the four different groups. When compared to the control group, the photoreceptor cell layer (VCL) was less compact and the

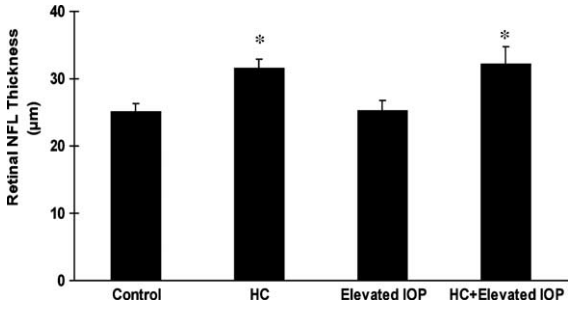

Fig. 1. Quantitative histologic measurements of retinal nerve fiber layer thickness in sections stained with toluidine blue. Values represent mean ± SD ($n = 9$). * $p < 0.01$ compared to control and elevated IOP group.

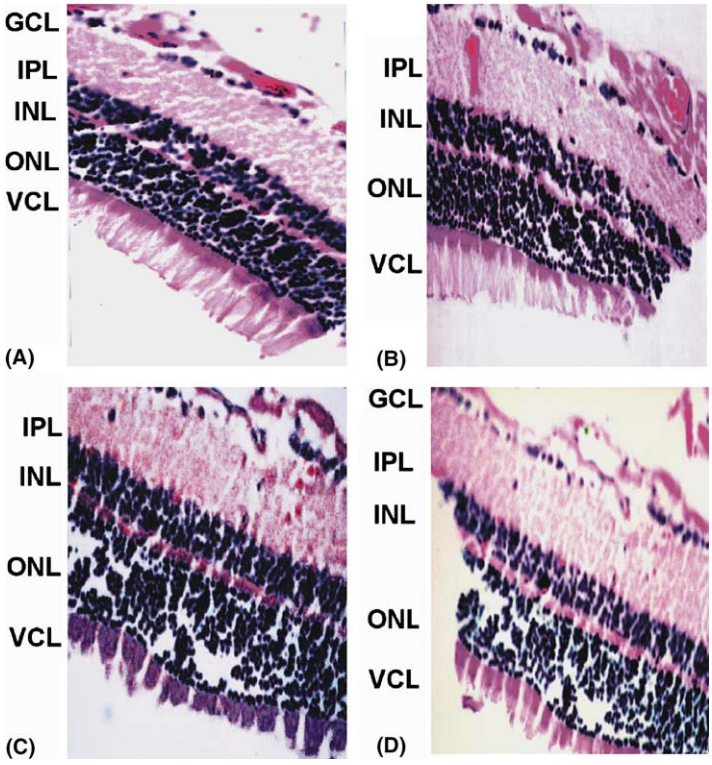

Fig. 2. Light microscopy of hematoxylin and eosin-stained paraffin sections of rat retinas. Photomicrographs of retinal sections of representative rat are shown from each of the four groups. (A) Control, (B) elevated IOP, (C) hypercholesterolemia and (D) hypercholesterolemia + elevated IOP. GCL, ganglion cell layer; IPL, inner plexiform layer; INL, inner nuclear layer; ONL, outer nuclear layer; VCL, photoreceptor cell layer.

Table 1
Number of cells in the outer nuclear and ganglion cell layer

Group	Cells/HPF[a]	
	ONL[b]	GCL[c]
Control	1046 ± 16.8	20.5 ± 0.3
HC[d]	813 ± 12.7*	16.9 ± 0.4*
Elevated IOP[e]	1051 ± 13.2	20.7 ± 0.2
HC[d] + Elevated IOP	804 ± 11.4*	16.6 ± 0.3*

* $p < 0.001$ compared to control and elevated IOP group.
[a] HPF—High Power Field (40×).
[b] ONL—outer nuclear layer.
[c] GCL—ganglion cell layer.
[d] HC—hypercholesterolemia.
[e] IOP—Intraocular pressure.Values represent mean ± SD ($n = 15$).

IPL/GCL appeared to be swollen, and increased in thickness in rats fed on high-cholesterol diet (Fig. 2C and D). Light microscopic observations of swelling were confirmed by morphometric analysis which quantified the cell numbers in both the ONL and GCL. As shown in Table 1, the number of cells/high power field (40×) were significantly reduced in rats fed on high-cholesterol diet, $p < 0.001$. Rats with only elevated IOP showed little or no structural abnormality (Fig. 2B).

3.4. Immunohistochemical analysis

Fig. 3 demonstrates the localization of NOS-2 in the retinal cross sections from representative rats of each of the four different groups. NOS-2 positive staining was observed throughout the OPL, IPL and GCL in rats with elevated IOP and/or hypercholesterolemia. The photoreceptor cell layer also showed diffuse NOS-2 immunostaining in elevated IOP and/or hypercholesterolemic rats. NOS-2 was not present in eyes of control rats. The quantitative data obtained for NOS-2 staining is shown in Fig. 4. When compared to the hypercholesterolemic and elevated IOP groups, NOS-2 immunostaining score as assessed in the VCL, IPL and GCL, was significantly greater in rats with hypercholesterolemia + elevated IOP ($p < 0.05$). NOS-2 immunostaining in elevated IOP was also significantly greater than in hypercholesterolemia alone ($p < 0.05$).

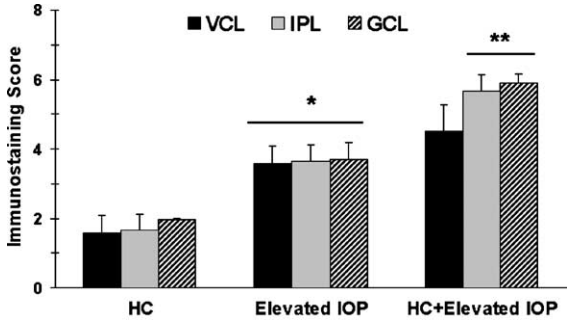

Fig. 4. Quantitation of NOS-2 immunostaining. Values represent mean ± SD ($n = 15$). The differences in the immunostaining score among the different groups were analyzed via Kruskal–Wallis one way analysis of variance on ranks and all pairwise multiple comparisons were performed by Dunn's method. * $p < 0.05$ compared to HC (hypercholesterolemia) and ** $p < 0.05$ compared to elevated IOP and HC.

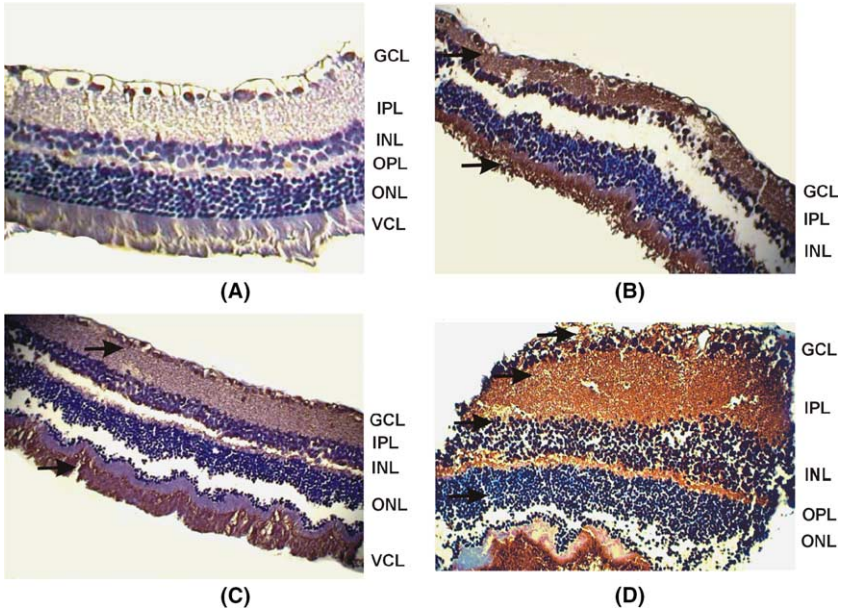

Fig. 3. Immunohistochemistry for NOS-2 in rat retinas. Photomicrographs of retinal sections of representative rat are shown from each of the four groups. (A) Control, (B) elevated IOP, (C) hypercholesterolemia and (D) hypercholesterolemia + elevated IOP. GCL, ganglion cell layer; IPL, inner plexiform layer; INL, inner nuclear layer; ONL, outer nuclear layer; VCL, photoreceptor cell layer. Arrows show regions of NOS-2 immunostaining.

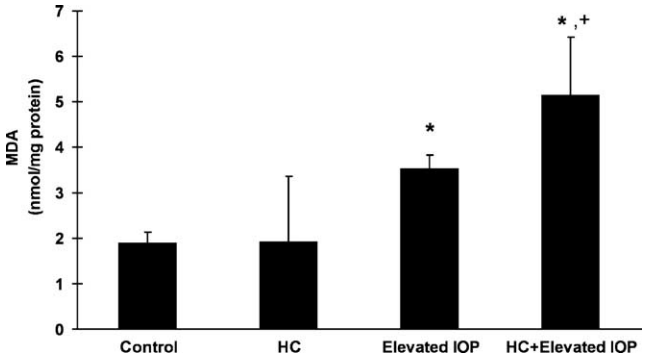

Fig. 5. Vitreous MDA levels. Values represent mean ± SD ($n = 6$). * $p < 0.05$ compared to control and hypercholesterolemia group. + $p < 0.05$ compared to elevated IOP group.

3.5. Lipid peroxidation

Vitreous MDA levels (mean ± SD, $n = 6$) detected in elevated IOP (3.51 ± 0.31 nmol/mg protein) and hypercholesterolemia + elevated IOP (5.14 ± 1.28 nmol/mg protein) groups were significantly higher ($p < 0.05$) than those detected in hypercholesterolemic (1.92 ± 1.43 nmol/mg protein) and control (1.89 ± 0.24 nmol/mg protein) groups. Vitreous MDA levels in rats with hypercholesterolemia + elevated IOP were also significantly greater ($p < 0.05$) than in rats with only elevated IOP (Fig. 5).

4. Discussion

This study examined the effect of high cholesterol on NOS-2 expression, lipid peroxidation and RNFL thickness in rats with elevated IOP. To accomplish this, rats were fed with laboratory chow supplemented with 4% (w/w) cholesterol, 1% cholic acid and 0.5% thiouracil for 24 weeks. This intake of cholesterol resulted in significantly elevated levels of serum cholesterol as reported previously (Deepa & Varalakshmi, 2004).

Although previous studies have determined the outcome of hypercholesterolemia on retinal vascular changes (Tomida, Tamai, & Matsuda, 2001; Yamakawa, Bhutto, & Lu, 2001) in rats, the effect of hypercholesterolemia and increased IOP on rat retinal morphology and structure has not been reported until now. The histological analysis of this investigation revealed diverse changes in the retinas of hypercholesterolemic rats after a 24-week feeding period. Light microscopic evaluation revealed that high-cholesterol caused breaks and discontinuation in focal areas in the ONL. VCL seemed less compact and the IPL/GCL appeared to be swollen, and increased in thickness in rats fed on high-cholesterol diet (Fig. 2). RNFL thickness in hypercholesterolemic rats was also significantly higher than those in the control and elevated IOP group (Fig. 1). Rats with hypercholesterolemia + elevated IOP were found to exhibit the most adverse changes in retinal structure and RNFL thickness suggesting that combination of hypercholesterolemia and increased IOP is additive in contributing to the pathogenic changes observed in the retinas of the reported rat model.

The observed increase in NOS-2 immunostaining in experimental rat models with elevated IOP and/or hypercholesterolemia is consistent with the involvement of NO neurotoxicity in elevated IOP and hyperlipidemia. Reported studies have demonstrated the presence of NOS-2 in glaucomatous optic nerve heads with consistent staining of nitrotyrosine, suggesting that reactive nitrogen species may contribute to retinal ganglion cell death associated with elevated IOP (Liu & Neufeld, 2000; Shareef et al., 1999). Indeed, pharmacological studies have shown that inhibition of NOS-2 by aminoguanidine provides neuroprotection of retinal ganglion cells in a rat model of chronic glaucoma (Neufeld, Sawada, & Becker, 1999). NOS-2 positive staining observed throughout the OPL, IPL and GCL (Fig. 3) is supportive of previous studies which have identified retinal NOS-2 production in pigmented epithelial cells (Goureau, Lepoivre, & Becquet, 1993), vascular endothelium (Chakravarthy, Stitt, & McNally, 1995) and Müller cells (Goureau, Hicks, & Courtois, 1994), that span the entire thickness of the retina.

Hypercholesterolemia plays an important role in endothelial dysfunction related to cardiovascular diseases. Recent studies have described increased NOS-2 immunoreactivity in aortic endothelial cells of Donryu rats on a cholesterol-enriched diet (Aliev et al., 2000). Similarly, increased expression of NOS-2 was reported in T-lymphocytes and macrophages of cholesterol-fed rabbits (Esaki, Hayashi, & Muto, 1997). Furthermore, it was demonstrated that a high-fat diet induced levels of NOS-2 mRNA in male Sprague-Dawley rats (Kim, Kang, & Oh, 2002). Increased retinal NOS-2 immunoreactivity observed in rats with hypercholesterolemia + elevated IOP (Fig. 4) is supportive of these findings and suggests that hypercholesterolemia may aggravate pathogenic changes in GON by stimulating the expression of NOS-2 and subsequent NO production.

Increased vitreous MDA levels detected in rats with elevated IOP (Fig. 5) is in agreement with previous reports that reveal the occurrence of oxidative stress in GON (Ferreira, Lerner, & Brunzini, 2004; Izzotti, Sacca, & Cartiglia, 2003). Oxygen radicals exert their cytotoxic effects, in part, by causing peroxidation of membrane lipids, which results in increased membrane permeability and the loss of membrane integrity (Freeman & Crapo, 1982). Increased cholesterol levels enhance the production of reactive oxygen species (ROS) and provoke cellular injury (White, Brock, & Chang,

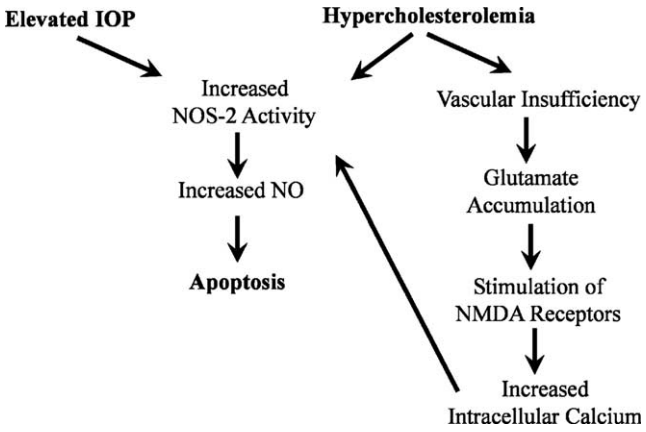

Fig. 6. The additive effects of hypercholesterolemia and elevated IOP on NOS-2 expression.

1994). Hypercholesterolemia stimulates the release of platelet-activating factor, which in turn increases the synthesis and release of inflammatory cytokines known to stimulate polymorph nuclear leukocytes to produce ROS (Prasad, Kalra, & Lee, 1994). The significant increase observed in vitreous MDA levels in rats with hypercholesterolemia + elevated IOP (Fig. 5) suggests that hypercholesterolemia is additive in contributing to oxidative stress and related pathogenic changes observed in the retinas of rats with elevated IOP.

In summary, the present data illustrates that both elevated IOP and hypercholesterolemia augments NOS-2 expression and leads to increased lipid oxidation in rats. Although these findings show increased IOP and cholesterol levels have additive effects on aforementioned parameters, it is unknown if they are related. Nevertheless, hypercholesterolemia is a risk factor in the development of GON (Hayreh et al., 1994; McGwin et al., 2004; Stewart et al., 1996; Tanaka et al., 2001; Winder, 1977) and as depicted in Fig. 6, data herein suggest that increased circulating cholesterol may exacerbate disease progression by inducing NOS-2 expression and elevating oxidant tissue injury.

Acknowledgment

This study was supported by a grant from Akdeniz University Research Foundation, Turkey (2003.01. 0103.007).

References

Aliev, G., Shi, J., Perry, G., et al. (2000). Decreased constitutive nitric oxide synthase, but increased inducible nitric oxide synthase and endothelin-1 immunoreactivity in aortic endothelial cells of donryu rats on a cholesterol-enriched diet. *Anatomical Record, 260*, 16–25.

Beckman, J. S., Beckman, T. W., Chen, J., et al. (1990). Apparent hydroxyl radical production by peroxynitrite: implications for endothelial injury from nitric oxide and superoxide. *Proceedings of the National Academy of Sciences USA, 87*, 1620–1624.

Becquet, F., Courtois, Y., & Goureau, O. (1997). Nitric oxide in the eye: multifaceted roles and diverse outcomes. *Survey of Ophthalmology, 42*, 71–82.

Chakravarthy, U., Stitt, A. W., McNally, J., et al. (1995). Nitric oxide synthase activity and expression in retinal capillary endothelial cells and pericytes. *Current Eye Research, 14*, 285–294.

Deepa, P. R., & Varalakshmi, P. (2004). Protective effects of certoparin sodium, a low molecular weight heparin derivative, in experimental atherosclerosis. *Clinica Chimica Acta, 339*, 105–115.

Esaki, T., Hayashi, T., Muto, E., et al. (1997). Expression of inducible nitric oxide synthase in T lymphocytes and macrophages of cholesterol-fed rabbits. *Atherosclerosis, 128*, 39–46.

Fechtner, R. D., & Weinreb, R. N. (1994). Mechanisms of optic nerve damage in primary open angle glaucoma. *Survey of Ophthalmology, 39*, 23–42.

Ferreira, S. M., Lerner, S. F., Brunzini, R., et al. (2004). Oxidative stress markers in aqueous humor of glaucoma patients. *American Journal of Ophthalmology, 137*, 62–69.

Flammer, J. (1994). The vascular concept of glaucoma. *Survey of Ophthalmology, 38*, S3–6.

Freeman, B. A., & Crapo, J. D. (1982). Biology of disease: free radicals and tissue injury. *Laboratory Investigation, 47*, 412–426.

Goldstein, I. M., Ostwald, P., & Roth, S. (1996). Nitric oxide: a review of its role in retinal function and disease. *Vision Research, 36*, 2979–2994.

Goureau, O., Hicks, D., Courtois, Y., et al. (1994). Induction and regulation of nitric oxide synthase in retinal Muller glial cells. *Journal of Neurochemistry, 63*, 310–317.

Goureau, O., Lepoivre, M., Becquet, F., et al. (1993). Differential regulation of inducible nitric oxide synthase by fibroblast growth factors and transforming growth factor beta in bovine retinal pigmented epithelial cells: inverse correlation with cellular proliferation. *Proceedings of the National Academy of Sciences USA, 90*, 4276–4280.

Greenfield, D. S. (1999). Glaucomatous versus nonglaucomatous optic disc cupping: clinical differentiation. *Seminars in Ophthalmology, 14*, 95–108.

Hayreh, S. S., Bill, A., & Sperber, G. O. (1994). Effects of high intraocular pressure on the glucose metabolism in the retina and optic nerve in old atherosclerotic monkeys. *Graefes Archive for Clinical and Experimental Ophthalmology, 232*, 745–752.

Hayreh, S. S., Pe'er, J., & Zimmerman, M. B. (1999). Morphologic changes in chronic high-pressure experimental glaucoma in rhesus monkeys. *Journal of Glaucoma, 8*, 56–71.

Heneka, M. T., Loschmann, P. A., Gleichmann, M., Weller, M., Schulz, J. B., Wullner, U., et al. (1998). Induction of nitric oxide synthase and nitric oxide-mediated apoptosis in neuronal PC12 cells after stimulation with tumor necrosis factor-alpha/lipopolysaccharide. *Journal of Neurochemistry, 71*, 88–94.

Hennis, A., Wu, S. Y., Nemesure, B., et al. (2003). Barbados eye studies group. Hypertension, diabetes, and longitudinal changes in intraocular pressure. *Ophthalmology, 110*, 908–914.

Hu, J., & Van Eldik, L. J. (1996). S100 induces apoptotic cell death in cultured astrocytes via a nitric oxide-dependent pathway. *Biochimica et Biophysica Acta, 1313*, 239–245.

Izzotti, A., Sacca, S. C., Cartiglia, C., et al. (2003). Oxidative deoxyribonucleic acid damage in the eyes of glaucoma patients. *American Journal of Medicine, 114*, 638–646.

Jonas, J. B., Budde, W. M., & Lang, P. (1998). Neuroretinal rim width ratios in morphological glaucoma diagnosis. *British Journal of Ophthalmology, 82*, 1366–1371.

Kim, Y. M., Bombeck, C. A., & Billiar, T. R. (1999). Nitric oxide as a bifunctional regulator of apoptosis. *Circulation Research, 84*, 253–256.

Kim, J. W., Kang, K. W., Oh, G. T., et al. (2002). Induction of hepatic inducible nitric oxide synthase by cholesterol in vivo and in vitro. *Experimental and Molecular Medicine, 34*, 137–144.

Klein, B. E., Klein, R., & Moss, S. E. (1984). Intraocular pressure in diabetic persons. *Ophthalmology, 91*, 1356–1360.

Liu, B., & Neufeld, A. H. (2000). Expression of nitric oxide synthase-2 (NOS-2) in reactive astrocytes of the human glaucomatous optic nerve head. *Glia, 30*, 178–186.

Lowry, O. H., Rosenbrough, N. J., Farr, A. L., et al. (1951). Protein measurement with folin-phenol reagent. *Journal of Biological Chemistry, 193*, 265–275.

McGwin, G., Jr., McNeal, S., Owsley, C., Girkin, C., Epstein, D., & Lee, P. P. (2004). Statins and other cholesterol-lowering medications and the presence of glaucoma. *Archives of Ophthalmology, 122*, 822–826.

Montoliu, C., Llansola, M., Monfort, P., et al. (2001). Role of nitric oxide and cyclic GMP in glutamate-induced neuronal death. *Neurotox Research, 3*, 179–188.

Neufeld, A. H., Sawada, A., & Becker, B. (1999). Inhibition of nitric-oxide synthase 2 by aminoguanidine provides neuroprotection of retinal ganglion cells in a rat model of chronic glaucoma. *Proceedings of the National Academy of Sciences USA, 96*, 9944–9948.

Prasad, K., Kalra, J., & Lee, P. (1994). Oxygen free radicals as a mechanism of hypercholesterolemic atherosclerosis: effects of probucol. *International Journal Angiology, 3*, 100–112.

Sarih, M., Souvannavong, V., & Adam, A. (1993). Nitric oxide synthase induces macrophage death by apoptosis. *Biochemical and Biophysical Research Communications, 191*, 508–509.

Sawada, A., & Neufeld, A. H. (1999). Confirmation of the rat model of chronic, moderately elevated intraocular pressure. *Experimental Eye Research, 69*, 525–531.

Shareef, S. R., Garcia-Valenzuela, E., Salierno, A., et al. (1995). Chronic ocular hypertension following episcleral venous occlusion in rats. *Experimental Eye Research, 61*, 379–382.

Shareef, S., Sawada, A., & Neufeld, A. H. (1999). Isoforms of nitric oxide synthase in the optic nerves of rat eyes with chronic moderately elevated intraocular pressure. *Investigative Ophthalmology & Visual Science, 40*, 2884–2891.

Stewart, W. C., Sine, C., Sutherland, S., & Stewart, J. A. (1996). Total cholesterol and high-density lipoprotein levels as risk factors for increased intraocular pressure. *American Journal of Ophthalmology, 122*, 575–577.

Sucher, N. J., Lipton, S. A., & Dreyer, E. B. (1997). Molecular basis of glutamate toxicity in retinal ganglion cells. *Vision Research, 37*, 3483–3493.

Tanaka, C., Yamazaki, Y., & Yokoyama, H. (2001). Study on the progression of visual field defect and clinical factors in normal-tension glaucoma. *Japan Journal of Ophthalmology, 45*, 117–121.

Tomida, K., Tamai, K., Matsuda, Y., et al. (2001). Hypercholesterolemia induces leukocyte entrapment in the retinal microcirculation of rats. *Current Eye Research, 23*, 38–43.

Wasowicz, W., Neve, J., & Peretz, A. (1993). Optimized steps in fluorometric determination of thiobarbituric acid-reactive substances in serum: importance of extraction pH and influence of sample preservation and storage. *Clinical Chemistry, 39*, 2522–2526.

White, C. R., Brock, T. A., Chang, L. Y., et al. (1994). Superoxide and peroxynitrite in atherosclerosis. *Proceedings of the National Academy of Sciences USA, 91*, 1044–1048.

Winder, A. F. (1977). Circulating lipoprotein and blood glucose levels in association with low-tension and chronic simple glaucoma. *British Journal of Ophthalmol, 61*, 641–645.

Yamakawa, K., Bhutto, I. A., Lu, Z., et al. (2001). Retinal vascular changes in rats with inherited hypercholesterolemia—corrosion cast demonstration. *Current Eye Research, 22*, 258–265.

Yamamoto, T., & Kitazawa, Y. (1998). Vascular pathogenesis of normal-tension glaucoma: a possible pathogenetic factor, other than intraocular pressure, of glaucomatous optic neuropathy. *Progress in Retinal and Eye Research, 17*, 127–143.

Yan, D. B., Coloma, F. M., Metheetrairut, A., et al. (1994). Deformation of the lamina cribrosa by elevated intraocular pressure. *British Journal of Ophthalmology, 78*, 643–648.